Nano World Journal

https://doi.org/10.17756/nwj.2024-s1-010

Review Article

Open Access

An Overview of Topological Insulators: Design, Types and Future Prospects

Anushka Banerjee*

Department of Physics, Jadavpur University, Kolkata, West Bengal, India

***Correspondence to:**
Anushka Banerjee
Department of Physics,
Jadavpur University,
Kolkata, West Bengal, India.
E-mail: ab14012001@gmail.com

Received: January 03, 2024
Accepted: March 06, 2024
Published: March 11, 2024

Citation: Banerjee A. 2024. An Overview of Topological Insulators: Design, Types and Future Prospects. *Nano World J* 10(S1): S48-S56.

Published by United Scientific Group

Abstract

Topological insulators (TIs) are one of the most promising prospects that are anticipated to herald in a new age in the field of electronic devices. They were experimentally found only a few years ago. These can be defined as electronic materials that behave like conductors along their surface but are insulating in the bulk. This paper provides an introductory perspective on TIs. A summary on the origin of TIs, their different types, designs, properties, challenges, and prospects are discussed. This paper also sheds light on a rich variety of theoretically predicted materials that could function as TIs.

Keywords

Topological insulators, Hall effect, Surface states, Spin-orbit coupling, Dirac fermions

Introduction

During charge transport, energy dissipation and scattering frequently happen. In the 1980s, the quantum Hall effect was realized in the electrons confined in two dimensions under a strong magnetic field. Along the sample boundary, currents were seen to flow without any dissipation. TIs were found to have similar metallic states which can be carried in the low-dissipation state [1]. Physics' definition of the term "topology" can be summarized as the properties of different systems that remain invariant despite the continuous deformations taking place in the system. In 2016, a new group of materials known as "TIs" were discovered. The name refers to the fact that they function as insulators within their bulk but have metallic surfaces. The metallic boundaries are present only when an insulator has defined topological invariants [2]. Ordinary insulators have a definite energy gap between the conduction and valence bands, which creates their non-conducting or insulating property. The surface states of an ordinary insulator are topologically trivial, that is they return to the same bulk band from where they had originated, say the conduction band, as depicted in figure 1a.

Under increasing spin-orbital coupling if the normal ordering of the conduction band and valence band is reversed, we get a TI. It is the inverted form of the bulk band that produces the metallic states. The band gap reduces, closes, and then reopens by anti-crossing [3]. Therefore, surface states that are gapless are present inside the bulk energy gap of a TI. These surface states generally show the dispersion of the type of Dirac cone in which spin and momentum are locked up and perpendicular to each other. Various materials such as HgTe and Bi_2Se_3 act as TIs [4]. Ordinary band insulators can also support conductive surface states. However, the gapless states of a topological insulator, are guarded by time-reversal symmetry. Therefore, non-magnetic disorders fail to destroy these states. The bulk valence and conduction bands are continuously connected by these surface

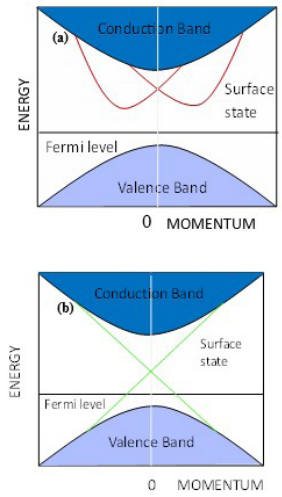

Figure 1: Schematic representation of the energy levels on the surface of a crystal as a function of surface crystal momentum for an **(a)** ordinary insulator and **(b)** TI.

states. An ordinary band insulator, whose Fermi level is contained within the conduction band and the valence band, has a structure that is comparable to that of the electronic band located in the bulk of a non-interacting TI. A TI's surface is home to special states that are located inside the bulk energy gap and allow for metallic conduction there. The metallic boundary states are topologically protected by an odd number of surface states. This is because the surface states connect the conduction band with the valence bands, and crossings at time-reversal-invariant points in the Brillouin zone [5]. Figure 1a and figure 1b show the difference between a conventional insulator and a TI. The lines represent the discrete edge or surface bands localized near the surfaces while the colored regions represent the bulk continuum states. For TIs, the surface bands always cross any Fermi level inside the bulk gap.

Historical Development

The quantum Hall state provided the first evidence of a topologically distinct state. In 1980, it was discovered that the bulk of the 2D sample of the quantum Hall state has an insulating nature and electric current could move only around the edges. This uni-directional current doesn't undergo dissipation and produces the quantum Hall effect (QHE) [5].

Earlier the QHE could be produced only in the presence of a magnetic field. This idea changed when in the late 1980s it was predicted that in 2D systems the motion of the electrons through the crystal lattice could produce quantum Hall states even without a macroscopic magnetic field.

Kane and Mele, in 2005, showed that the quantum spin Hall (QSH) effect still survived without a conserved spin current. They became aware of the possibility of actual 2D materials containing an edge state that is stable even in the absence of a magnetic field. Spin-orbit coupling (SOC) has the effect of producing these alike edge states. Hence, this final state in 2D was the first TI to be realized [2].

Graphene contains a honeycomb carbon lattice structure. One atomic layer of this lattice was fabricated. A tiny bulk gap was observed at the Dirac point in the electronic bulk structure of graphene which was created by the intrinsic SOC in graphene. This small gap transformed graphene to a gapped state from a gapless semimetal. Hence, graphene was the first 2D TI found to contain the QSH effect. However, the feeble SOC of graphene prevented the experimental verification. This is because the bulk energy gap created in it by the weak SOC is extremely small. Different methods have been suggested to increase the SOC like heavy atom doping [6].

2D TIs

Nanomaterials having two 2D TI materials were first experimentally discovered by the Bernevig-Hughes-Zhang (BHZ) model. In the year 2006, electronic band inversion helped to generate TIs. In this process, the general ordering of conduction and valence band was reversed with the help of the relativistic effect. This mechanism aided the TI states in the nanomaterials to be present in different kinds of materials having stronger SOC. Hence, this process helped in the growth of newer 2D TI materials. From both the BHZ mechanism and the Kane-Mele model, it can be concluded an energy gap is present in the 2D bulk of all QSH insulators. The metallic edge states bridge the gap in the bulk and counter-propagating on the boundary are two sets of edge states having spin polarization in the opposite direction. Figure 2 shows the schematic representation of the 1D edge states present in a 2D TI. The opposite spin character of the edge states is represented by the red and blue curves.

Unlike graphene, the QSH state and the topologically non-trivial gap (10 meV) in HgTe/CdTe quantum well (QW) are quite large for verifying experimentally. The Kane-Mele and BHZ models provide two definite approaches corresponding to two generalized routes for understanding 2D TIs theoretically. The Kane Model proposes the opening of a bulk band gap at two inequivalent Dirac points by SOC and the 2D TIs falling under this category are known as type I 2D TIs. However, the BHZ model deals with the realization of 2D TIs by inducing band inversion via SOC in 2D semiconductors and these are known as type II 2D TI.

The forerunner of type I 2D TI is graphene. The graphene-based TI model has generalized a large family of 2D materials with lattices with a honeycomb topology. Unlike type I 2D TI, the structures of type II 2D TI are not restricted to a honeycomb lattice. When compared to theoretical advancements,

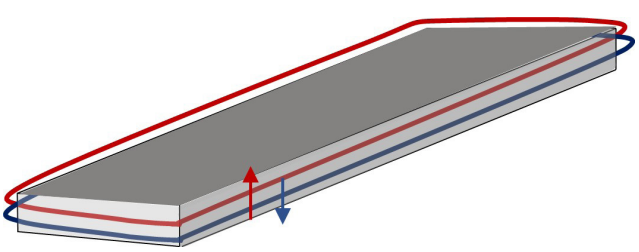

Figure 2: 2D TIs.

the experimental advancements in the field of 2D TIs are less significant. HgTe/CdTe QW is the first 2D TI described experimentally in the year 2007 [6].

Topological phases in 2D Tis

The different topological phases shown by these 2D TIs at the nanoscale are as follows:

Quantum Hall phase

In the year 1980, this phase was identified for the first time. It was discovered that a 2D electron gas displays a quantized Hall conductance in the presence of a magnetic field perpendicular to its direction of travel [7]. In this phase, the electrons are concentrated in the bulk but travel in one direction along the borders as depicted in figure 3 (top). The broken time-reversal symmetry induces chirality in the transportation of edge modes. This means that the electrons travel either clockwise or in the anti-clockwise direction. Furthermore, the electrons cannot travel in the reverse direction as indicated by the specific sign of the group velocity (Figure 3 (bottom)). Hence, the edge states are not back-scattered even in the presence of big defects. The green line in figure 3 represents the states present along the edge in this phase.

QSH phase

Kramer's theorem tells that, for a system containing half-integer spin, all eigenstates must be at least doubly degenerate under time-reversal symmetry. The spin-up electrons encounter different forces, unlike the spin-down electrons under SOC. Despite the degeneracy in the energy level, the two sets of electrons may depict dissimilar topological behavior. This means that if spin-up electrons travel in the clockwise direction along the boundary then the spin-down electrons will propagate in the anti-clockwise direction or vice versa. This has been depicted in figure 4 (top). For each spin, the edge states present in the band gap of a QSH insulator are gapless while the sign of their group velocity is locked by the spin, as depicted in figure 4 (bottom). This state can be contemplated as dual copies of the quantum Hall state for a spin [8].

Quantum valley Hall phase

A valley denotes momentum with an extremum in the local energy. At a valley, if a Dirac point is lifted, then the band gap may support this phase. In this phase, the electrons at separate valleys travel in the opposite direction along the boundaries, as depicted in figure 5 (top). The dispersion of the edge state of a quantum valley Hall insulator shows reverse signs of the group velocity, as depicted in figure 5 (bottom) [8].

Floquet topological phase

This phase is a time equivalent of the Bloch theorem. The Floquet theorem tells that multiplying a phase term by a function that is periodic in time aids in expressing the solution of a time-periodic Hamiltonian. This theorem aids in the study of quantum systems that are driven periodically. A system under the influence of periodic temporal modulation can assist a topological phase known as the Floquet topological phase.

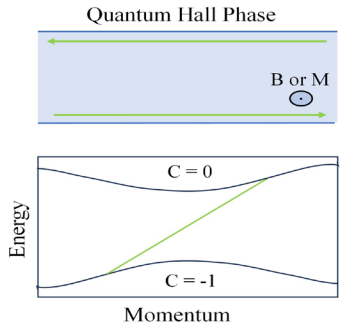

Figure 3: Schematic representation of the edge states in quantum Hall phase.

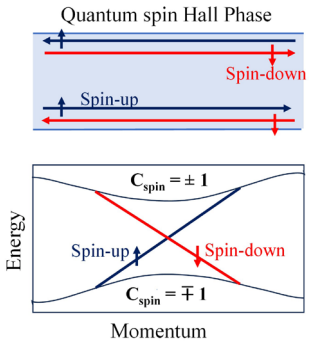

Figure 4: Schematic representation of the edge states in QSH phase.

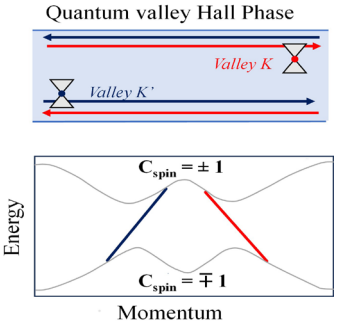

Figure 5: Schematic representation of the edge states in quantum Hall phase.

Zak phase

Integration of the Berry connection along the axis of one wave vector aids in acquiring this phase. It can be observed as the Berry phase in 1D. The topology of this phase arises in bulk polarization or by the shift of the Wannier band. The edge modes of a 2D system that bring the non-trivial Zak phase float inside the band gap and are not attached to the bulk bands. However, the topological protection of this phase is weaker than the other phases. Unlike the phases discussed above the ordinary insulating phase does not contain conducting edge states (Figure 6).

Examples of 2D TIs

The BHZ model was basically inspired by the CdTe/HgTe/CdTe QW which contains an inversion between the s- and p- orbitals at wave vector, k = 0 as a function of the width of the well. Hence, as per the BHZ model, this inver-

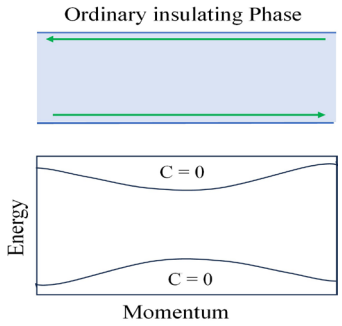

Figure 6: Schematic representation of the edge states in the ordinary insulating phase.

sion is necessary to acquire a TI nature. This band inversion is realized only by bulk HgTe and not by CdTe. In the band structure of bulk HgTe, however, the semiconductor band gap is intrinsically zero because of a crystal symmetry whose degeneracy is protected at the Γ point. Hence, no band gap exists between the s and p-orbitals; thus, the system cannot be called an insulator. The lattice constant of CdTe is somewhat higher. On sandwiching it with HgTe, the cubic lattice symmetry of HgTe breaks and opens a gap creating a proper insulator. The BHZ model was predicted and later, experimentally verified that the strained HgTe unit retains the band inversion only above a particular critical thickness and can be then regarded as a TI [9].

For the experimental verification, molecular beam epitaxy was implemented, and the topological quantum phase transition had a critical thickness of around 6.3 nm. The sample was found to have an inverted band (i.e., a negative energy gap), and the quantized Hall conductance was measured to be $2e^2/h$ without any magnetic field. The chemical potential was tuned into the gap. The nontrivial gap of 10 meV being small, rendered this prototype 2D TI convenient only for laboratory demonstration but unsuitable for real applications. Below the critical thickness, the band inversion did not exist and a diverge in the resistivity was also observed.

The one drawback of the CdTe/HgTe/CdTe QW was that the bulk band gap created by the epitaxial strain was up to the order of 10 meV (depending on the thickness) i.e., it was very small and hence the TI phase could be detected only at extremely low temperatures. AlSb/InAs/GaSb/AlSb QW was another theoretically predicted and experimentally verified 2D TI system recently discovered.

The strong SOC of Bi (approx. 1 eV) indicates Bi-containing compounds to be promising candidates for TIs. Hence the binary compositions of group III elements (B, Al, Ga, In, and Tl) and Bi having a buckled honeycomb structure have been theoretically predicted to be potential candidates for acting as 2D TIs [10].

A total of 6 compounds GaBi, InBi, TlAs, TlBi, TlSb, and TlN are theoretically proposed to have a topologically nontrivial band gap. However, their dynamical and thermal stability have not been checked using phonon and molecular dynamics simulations due to which the stability of their structure is still uncertain. In these hexagonal structures, each atom X (Ga, In, Tl) bonds with three Bi atoms only. Possibly these structures can be stabilized by surface passivation or substrates [6].

Recently 2D transition-metal carbides M_2C, have been discovered [11]. They are known as Mxenes. These are layered materials that can be exfoliated from bulk materials. Furthermore, functionalized Mxenes with oxygen M_2CO_2 (M = W, Mo, and Cr) constitute a newly discovered family of 2D TIs. The band inversion inside these 2D TI materials occurs among the bonding and anti-bonding orbitals of M d orbitals.

A strong SOC which is one of the main factors in creating a TI is generated either from the component of a constituent material or from other external sources such as doping or proximity effect. However, there are no limitations on the specific form of the constituent material. In fact, QSH states are found even in organic materials. For example, covalent organic frameworks which contain heavy metals like Pb and Bi are organic 2D TIs. Moreover, a family of organic 2D TIs in organometallic lattices, $Pb(C_6H_5)_3$ and $Bi(C_6H5)_3$ have been predicted by first-principal calculations. Furthermore, on replacing Bi or Pb atoms with magnetic elements like Mn, a quantized Hall conductivity is produced by the effects of spontaneous magnetization and SOC [6].

The quantized Hall conductivity coupled with broken time-reversal symmetry forms a family of 2D organic TIs that aids in realizing the concept of the quantum anomalous Hall effect (QAHE). Despite the importance of SOC in band inversion and producing the associated QSH, there are other ways by which this can be made possible. For example, in the 2D TI material $ZrTe_5/HfTe_5$. The conduction and valence bands meet at the Fermi level and a topologically trivial band gap is opened by the SOC without any band inversion. The band inversion that occurs is due to band splitting which is created by the non-symmorphic features of the space group of the material [6].

3D TIs

In 2D TIs, the insulating gap in the gapless and bulk states of the QSH state contains counterpropagating opposite spin states. These two opposite spin states form one massless Dirac fermion at the edge. The crossing of their dispersion branches at a time-reversal invariant point is secured by time-reversal symmetry. Massless, 2D Dirac fermions were experimentally discovered in graphene such that each of the spin orientations had two inequivalent massless Dirac points. Hence four copies of massless Dirac fermions can be found in all. Each Dirac fermion produces a Hall conductance of $e^2/2h$ (h stands for Planck's constant) in an external magnetic field. Hence, it matches the experimental value of quantized Hall conductance which is $2e^2/h$. Time-reversal invariant purely 2D free fermion systems cannot have a single or odd number of massless Dirac fermions. Therefore, graphene contains an even number of massless Dirac fermions. However, one Dirac fermion can occur in 2D time-reversal invariant systems in the boundary of a 3D topological insulator [12], which contains a bulk insulating gap and an odd number of gapless Dirac cones on the surface.

Hence, 3D TIs can be defined as newly discovered states of quantum matter with a bulk gap and an odd number of Dirac fermions on the surface. The topological order or exotic quantum entanglement of 3D TIs is predicted to create unusual conducting 2D surface states having novel spin-selective energy-momentum dispersion relations. Figure 7 shows the schematic representation of the 2D surface states present in a 3D TI. The opposite spin character of the surface states is represented by the red and blue curves.

The first experimentally identified 3D TI was the alloy $Bi_{1-x}Sb_x$ which had a semiconducting nature and whose unique surface bands were experimentally mapped in an angle-resolved photoemission spectroscopy (ARPES) experiment. However, $Bi_{1-x}Sb_x$ had a rather complicated surface structure with a small band. These problems led to the realization of second-generation 3D TI materials. A family of stoichiometric materials, Bi_2Se_3, Bi_2Te_3, and Sb_2Te_3, were theoretically predicted, to be the simplest 3D TIs with one Dirac cone at the Γ point of their surface states. In 2008, the surface band structure of Bi_2Se_3 was studied with the help of ARPES and first principal calculations. It was observed that they form a single Dirac cone and hence act as TIs. Additionally, theoretical studies used electronic structure to prove that Bi_2Se_3 has a large band gap. Experimentally, the surface state of Bi_2Te_3 (1) and Sb_2Te_3 (2) were also found to contain a single nondegenerate Dirac cone. This was done with the help of ARPES [13].

These 2D and 3D TIs i.e., HgTe, Bi_2Te_3, Bi_2Se_3, and Sb_2Te_3 facilitate the discovery of newer TIs. The non-trivial topological property of TIs originates due to the inverted band structure induced by SOC. Therefore, the probability for materials containing compounds with covalent bonds having narrow band gaps and heavy atoms with a high SOC to behave like TIs is more. These ideas have led to the discovery of many new TIs, some of which have been theoretically proposed while others have been experimentally synthesized and characterized [5].

Photonic topological phases in 3D TIs

3D gapped phase

The 3D phases can be obtained by the extension of the topological insulating phases in 2D via a 2D crystalline structure that comprises periodically arranged unit cells along all three spatial directions. The 3D band gap in these 3D gapless topological phases separates the topologically inequivalent bands. Gapless surface states are observed to emerge inside the band gap when one of the two topologically distinct 3D bulk bands is present above the band gap while the other one is present below it. A 3D photonic gapped phase allows photons to travel firmly against the defects along any spatial direction without being confined to a certain plane. This phase is also called the topological insulating phase in 3D.

3D gapless phase

This phase has been discovered recently and can be referred to as the topological semi-metal phase. There are no 2D counterparts of these phases, unlike the 3D gapped phase. These phases are identified by Weyl degeneracies (that is, degeneracy existing amidst topologically inequivalent bands) in the place of a band gap. A Weyl point which is a Weyl degeneracy of 0D is the main characteristic of this phase.

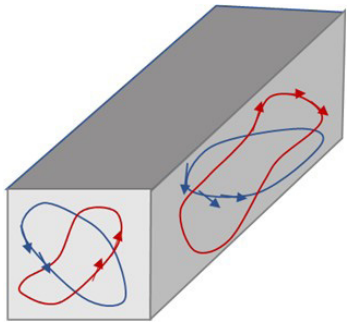

Figure 7: 3D TI.

Candidate 3D Tis

There exist other theoretically predicted 3D TIs whose topological surfaces have not been experimentally discovered. A few of these have been listed below:

Ag_2Te

It has been predicted that the linear-in-B magnetoresistance of this material is large over an extremely wide magnetic field range. This property has been predicted to have connections with its 3D TI characteristics [14]. No ARPES measurements have been yet reported about this material. However, Aharovan-Bohm oscillations have been seen in Ag_2Te nanowires which gives light to the existence of some conduction layers on the surface. However, the topological nature of this material has not yet been confirmed.

SmB_6

This material has been predicted to be a topological Kondo insulator since the band gap of the material arises from the Kondo effect [15]. Proofs of surface-dominated transport at lower temperatures in this material have been reported. However, the current ARPES data fail to indicate a topological surface state within a small band gap (~20 meV) [16].

$Bi_{14}Rh_3I_9$

This is another predicted weak 3D TI. The *ab initio* band calculations predict that this material is a quasi-2D system consisting of stacked layers of 2D TI. Hence, it is predicted that the material could serve as a weak 3D TI. The difference between 2D and 3D TIs is shown in table 1 and the difference between weak and strong TIs is shown in table 2

Preparation of TIs

Mechanical exfoliation

The molecular structure of 3D TIs is distinctive. The fundamental quintuple layer, for instance, is made up of two Bi atoms and three Se atoms in the case of Bi_2Se_3. The Van der Waals force, a weak intermolecular force, holds each of the two quintuple layers together. The crystal between the layers

Table 1: Difference between 2D and 3D TIs.

2D TI	3D TI
They have a large band gap in the bulk	They have a comparatively moderate band gap (0.35 eV)
They have limited applications	These are more promising since their stoichiometry is relatively stable
Their electronic state is the 1D edge	The topological state in this case is 2D
Example: $Hg_{1-x}Cd_xTe$	Examples: Bi_2Se_3, Bi_2Te_3 and Sb_2Te_3

Table 2: Difference between weak and strong TIs.

Weak TI	Strong TI
There are an even number of Dirac points in the surface Brillouin zone.	There are an odd number of Dirac points in the surface Brillouin zone.
The electrons can get localized on the surface due to strong disorders.	Non-magnetic disorders on the surface do not affect the localization of electrons. Hence, they have perfect metallic states.
Example: Sb_2Se_3	Examples: Bi_2Se_3, Bi_2Te_3 and Sb_2Te_3

is easily separated by the external force [17]. Graphene, for example, is prepared by stripping the layers of graphite. In the year 2010, ultra-thin Bi_2Se_3 films were produced by this method. In a similar way, exfoliating TI can produce TI layers. In 2010, it was found that mechanical exfoliation also helped in improving and stacking the thermoelectric properties of the thin films of TI (Figure 8).

Molecular beam epitaxy (MBE)

MBE is a crucial component of today's epitaxial growth technology. MBE is used to create photoelectric and semiconductor thin films. Under extremely high vacuum, one or more molecular beam or thermal atom components are injected onto the heated substrate's surface. One crystal film is deposited once the substrate's surface reacts with it. The molecular beam will suffer surface migration, adsorption, and nucleation after exchanging energy with the substrate. A film will eventually come into being. Physical and chemical changes both take place throughout this process. During the formation process, the compound and substrate are combined. In 2011, a study was conducted on the growth of TI, Bi_2Te_3 on Si (111) substrate [18]. It was also revealed that using the MBE process, it is possible to create undoped Bi_2Te_3 films with varied carriers at various growth temperatures. It showed that the n-type and p-type could be made under 590 K and 630 K temperatures respectively. Controlling the growth rates helped to lessen the material's flaws. Improving the growing conditions may also increase the material's mobility.

Chemical vapor deposition (CVD)

To prepare high-quality TIs, CVD is used. This method can produce ribbon, linear, and sheet-like nanomaterials. Due to high temperature, the reactant evaporates. The produced material then collects on the surface of the heated substrate through the transmission of gas. A broad area of the material can be fabricated with this method. CVD undergoes both phase

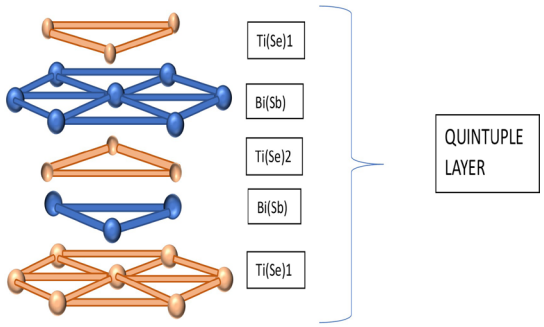

Figure 8: The quintuple layer of TIs.

and chemical changes. The gas-liquid-solid phase method is the main technique of this process. Multilayer, high-quality Bi_2Se_3 film with elongated, hexagonal, asymmetric structure is fabricated using CVD. CVD was also used to make ultrathin $Pb_{1-x}Sn_xTe$ nanoplates (40 nm) on SiO_2/Si substrate in the year 2016 [19].

Solvothermal synthesis

This is one of the new-generation methods used to prepare nanomaterials that are developed by the hydrothermal method. Due to the catalyst present in the tightly enclosed container, the substance within the fluid grows towards nucleation. Under high pressure and temperature circumstances, this happens. It eventually crystallizes to form nanomaterials. Solvothermal synthesis involves the use of non-aqueous or organic solvents such alcohols and organic amines. Sb_2Te_3/Bi_2Te_3 horizontal heterojunctions were created in 2015 utilizing a two-step solvothermal synthesis process [20]. Additionally, this technique aids in doping throughout the creation process. By using this technique, layered S-doped Bi_2Se_3 microspheres were created. These microspheres were collected from nanosheet stacks.

Metal organic chemical vapor deposition (MOCVD)

Vapor phase epitaxy has led to the development of a novel technology called MOCVD. It is a method of ultrafine processing used to create single crystal and semiconductor films. For the growth of the crystals, source materials such as organic compounds from Groups II and III, hydrides from Groups V and VI, are employed. The thermal decomposition reaction performs gas phase epitaxy on the surface, leading to the growth of single crystal films and semiconductors. 10 μm long ultra-thin Bi_2Se_3 single crystal nanoribbons have been prepared using MOCVD. This length could be about three to four times the length obtained from solvothermal synthesis. In 2012, MOCVD was used to fabricate thin films of wafer-scale Bi_2Te_3 on the substrate of GaAs (001), and its electrical properties were measured. Additionally, there are other methods of synthesis as well. Some of these include the vapor-liquid-solid method and vapor-solid growth methods.

After preparing the TIs, the next step is their identification. They can be identified using ARPES or scanning tunneling microscope techniques. X-ray diffraction and energy dispersive spectroscopy can be used for further measurements.

Doping frequently enhances the characteristics of TI. For instance, the thermoelectric characteristics of Bi_2Se_3 and the mobility of its surface electrons can both be improved by the right amount of doping. The doping impurities can be separated into two types. These comprise non-magnetic substances like Ag and Ga as well as magnetic substances like Fe and Mn. The safety provided by time-reversal symmetry can be destroyed by magnetic impurities, which can widen the band gap of surface states. As a result, phenomena like magnetic monopoles and QAHE [1] are possible. However, the non-magnetic impurities have relatively little effect on TI because of the time-reversal symmetry. Doping the TIs can change both the type of charge carriers and the concentration of TI. The band gap and Dirac point of the TIs are essentially affected by these doping impurities. Doping typically takes place as the material is being made. However, preserving the surface states of the TI during doping presents challenges.

Characteristics of TIs

Linear dispersion between the energy and momentum is a characteristic of TIs, like a propagating photon. Due to their extreme sensitivity to the external electric field, TIs have a nature that helps semiconductor devices function better [17].

The carriers present in an ideal TI have a high mobility which is the produced drift velocity under the influence of an electric field having a magnitude of unity. Practically, high mobility increases the running speed and cut-off frequency of a TI-based device.

TI also has a low-power dissipation, which allows for the operation of low-power TI-based devices. Resistance in conductors results from electron collisions with impurities, phonons, and other particles, whereas resistance in insulators results from the presence of band gaps. The surface of the TI has a Dirac electron that can move past the impurity and continue in its original path while meeting it. The spin orientation also reverses as the electron moves in both clockwise and anti-clockwise directions when it meets the impurity. To avoid the contaminants, the two scattering waves coherently cancel one another. This substantially lowers the resistance. The insulator within lessens electrical leakage. Thus, the TI based gadgets function at a minimal power [17].

The spin-polarized structure and spin-momentum locking is found in the electrons on the TI's surface. Because there are electrons with both up and down spins, the degree of freedom also grows. TIs can therefore be utilized to explore magnetic and spin-electronic devices.

Experiments of QSH can be performed on the surface state of TIs. In fact, the half-integer quantum Hall effect, magnetic monopole, and fractional charge can also be studied using TIs.

TI Nanostructures

Studying the transport properties of TIs in bulk crystals is not easy. This is because of the residual bulk carriers due to which the impact of the surface states to transport becomes very less. On the other hand, nanomaterials have enhanced surface states because of a high surface-to-volume ratio which aids in studying the topological properties of the surface states. TI nanostructures provide many advantages compared to the TIs in bulk crystals. Today, many nanostructures like nanoribbons and nanoplates are being fabricated from TIs. TI nanostructures have cross-sections that mirror the symmetry of the underlying crystal structure. These nanostructures have clearly established morphology at the nanoscale. This leads to transport circumstances that drive TI surface electrons to follow an established path at the nanoscale, which is perfect for experiments on TI surface electrons like Aharonov-Bohm oscillations [21].

Challenges

The current challenge in this field is the rapid destruction of the surface states, whenever the TIs are kept in contact with air. Problems of surface oxidation and the appearance of other adatoms largely diminish the surface state's movements. It increases the number of extra electron carriers which dominate transport [22]. Furthermore, when TIs are kept for a long time in the air, it leads to the formation of 2D electron gas as well [23]. This makes it difficult to analyze the actual states of TI. These problems have been resolved to some extent by *ex-situ* coating of nanostructures. For instance, when nanoribbons of Bi_2Se_3 are coated by sputtering ZnO on them, they show, that the carrier density was found to be minimum [24].

Applications and Future Prospects of TIs

The most dominant applications of TIs are in the fields of electronics and optoelectronics. The inhibition of backscattering of the surface states corresponding to unusual mobility in propagation and decreased energy consumption is an essential factor in semiconductor devices. TIs are also used in spintronics. The rare spin texture causes the charge current present on the surface of the TI to automatically supply a resultant spin density which makes them important in memory devices and spin-torque devices. Recently, several phase-changing memory materials are also being used as TIs. [1]. TI can also be used as dissipative transistors for quantum computers based on QHE and QAHE.

TIs are also supposed to have potential applications in catalytic chemistry. Recently, a study has predicted that TI flakes covered with noble metals would show improved catalytic activity in some reactions [25]. Hence, TI can be regarded as one of the most encouraging magnetic, optoelectronic, semiconductor, and quantum materials with exceptional magnetic, optical, and electrical properties.

Today, TIs are being used in photodetectors, magnetic devices, field effect transistors, and lasers. TIs will surely dominate in major scientific areas as well as in day-to-day activities soon. However, many challenges persist in this field which in turn increases the demand for further research. Any ideal TI material has a high mobility of surface electrons. However, due to the various existing limitations in the methods of preparation of TIs, there are inevitably defects present in the TIs

due to which the actual parameters become lesser compared to the theoretical values. This limits the practical applications of 2D TIs [17]. The defects in the material create a large bulk conductance. The synthesis and characterization of 2D TIs is still difficult and that increases the necessity for innovation and breakthrough.

The unique properties of the 2D and 3D TIs increase their demand in the field of nanoscience. They are predominantly being used in nanodevice fabrication based on topological surface state. They are used in the synthesis of nano-structuring techniques to create nano-sized domains with distinct topological characteristics and electronic properties [26]. Topological nanowires and nanoribbons come with unique electronic states at the edges with novel transport and quantum confinement effects [27]. Integrating TIs in quantum dots enable controlling lights at the nanoscale [28]. The spintronic effects of the topological insulators can be used to design nanoscale spintronics that can leverage the protected surface electrons [29]. These examples prove that the topological insulators, both in 2D and 3D offer several unique electronic properties which can offer breakthroughs in nanotechnology.

In the future TIs can be used to develop nanoscale heterostructures with superconductors that can benefit from Majorana fermions as well [30].

Researchers have found that enhancing the preparation methods and using highly accurate equipment's aid in fabricating highly pure single-crystal TI. Doping also helps in enhancing the properties of TIs by varying the Fermi level, concentration, and type of carriers in the TI. Moreover, various magnetic and non-magnetic impurities introduce superconductivity, magnetic monopole, and QAHE in the TIs. There exist various undiscovered features of TIs in quantum Hall states; the findings of quasi-particles with modified charges and statistics are the most important ones. TIs have also been predicted to occur in frustrated spin systems. There are many different types of TIs that are yet to be discovered [2]. It can be expected that this field will experience rapid growth and offer ample research opportunities in the future.

Acknowledgments

None.

Conflict of Interest

None.

References

1. Kong D, Cui Y. 2011. Opportunities in chemistry and materials science for topological insulators and their nanostructures. *Nat Chem* 3(11): 845-849. https://doi.org/10.1038/nchem.1171
2. Moore JE. 2010. The birth of topological insulators. *Nature* 464(7286): 194-198. https://doi.org/10.1038/nature08916
3. Wang X, Bian G, Miller T, Chiang TC. 2013. Topological quantum well resonances in metal overlayers. *Phys Rev* 87(23): 235113. https://doi.org/10.1103/PhysRevB.87.235113
4. Yan B, Felser C. 2017. Topological materials: Weyl semimetals. *Annu Rev Condens Matter Phys* 8: 337-354. https://doi.org/10.1146/annurev-conmatphys-031016-025458
5. Qi XL, Zhang SC. 2011. Topological insulators and superconductors. *Rev Modern Phys* 83(4): 1057. https://doi.org/10.1103/RevModPhys.83.1057
6. Kou L, Ma Y, Sun Z, Heine T, Chen C. 2017. Two-dimensional topological insulators: progress and prospects. *J Phys Chem Lett* 8(8): 1905-1919. https://doi.org/10.1021/acs.jpclett.7b00222
7. Klitzing KV, Dorda G, Pepper M. 1980. New method for high-accuracy determination of the fine-structure constant based on quantized Hall resistance. *Phys Rev Lett* 45(6): 494. https://doi.org/10.1103/PhysRevLett.45.494
8. Kim M, Jacob Z, Rho J. 2020. Recent advances in 2D, 3D and higher-order topological photonics. *Light Sci Appl* 9(1): 130. https://doi.org/10.1038/s41377-020-0331-y
9. Bernevig BA, Hughes TL, Zhang SC. 2006. Quantum spin Hall effect and topological phase transition in HgTe quantum wells. *Science* 314(5806): 1757-1761. https://doi.org/10.1126/science.1133734
10. Chuang FC, Yao LZ, Huang ZQ, Liu YT, Hsu CH, et al. 2014. Prediction of large-gap two-dimensional topological insulators consisting of bilayers of group III elements with Bi. *Nano Lett* 14(5): 2505-2508. https://doi.org/10.1021/nl500206u
11. Naguib M, Kurtoglu M, Presser V, Lu J, Niu J, et al. 2011. Two-dimensional nanocrystals produced by exfoliation of Ti_3AlC_2. *Adv Mater* 23(37): 4248-4253. https://doi.org/10.1002/adma.201102306
12. Fu L, Kane CL, Mele EJ. 2007. Topological insulators in three dimensions. *Phys Rev Lett* 98(10): 106803. https://doi.org/10.1103/PhysRevLett.98.106803
13. Chen YL, Analytis JG, Chu JH, Liu ZK, Mo SK, et al. 2009. Experimental realization of a three-dimensional topological insulator, Bi_2Te_3. *Science* 325(5937): 178-181. https://doi.org/10.1126/science.1173034
14. Zhang W, Yu R, Feng W, Yao Y, Weng H, et al. 2011. Topological aspect and quantum magnetoresistance of β-Ag_2Te. *Phys Rev Lett* 106(15): 156808. https://doi.org/10.1103/PhysRevLett.106.156808
15. Dzero M, Sun K, Galitski V, Coleman P. 2010. Topological Kondo insulators. *Phys Rev Lett* 104(10): 106408. https://doi.org/10.1103/PhysRevLett.104.106408
16. Miyazaki H, Hajiri T, Ito T, Kunii S, Kimura SI. 2012. Momentum-dependent hybridization gap and dispersive in-gap state of the Kondo semiconductor SmB_6. *Phys Rev* 86(7): 075105. https://doi.org/10.1103/PhysRevB.86.075105
17. Tian W, Yu W, Shi J, Wang Y. 2017. The property, preparation, and application of topological insulators: a review. *Materials* 10(7): 814. https://doi.org/10.3390/ma10070814
18. Krumrain J, Mussler G, Borisova S, Stoica T, Plucinski L, et al. 2015. MBE growth optimization of topological insulator Bi_2Se_3 films. *J Cryst Growth* 324(1): 115-118. https://doi.org/10.1016/j.jcrysgro.2011.03.008
19. Wang Q, Cai K, Li J, Huang Y, Wang Z, et al. 2016. Rational design of ultralarge $Pb_{1-x}Sn_xTe$ nanoplates for exploring crystalline symmetryβ protected topological transport. *Adv Mater* 28(4): 617-623. https://doi.org/10.1002/adma.201504630
20. Fei F, Wei Z, Wang Q, Lu P, Wang S, et al. 2015. Solvothermal synthesis of lateral heterojunction Sb_2Te_3/Bi_2Te_3 nanoplates. *Nano Lett* 15(9): 5905-5911. https://doi.org/10.1021/acs.nanolett.5b01987
21. Aharonov Y, Bohm D. 1959. Significance of electromagnetic potentials in the quantum theory. *Phys Rev* 115(3): 485. https://doi.org/10.1103/PhysRev.115.485
22. Kong D, Dang W, Cha JJ, Li H, Meister S, et al. 2010. Few-layer nanoplates of Bi_2Se_3 and Bi_2Te_3 with highly tunable chemical potential. *Nano Lett* 10(6): 2245-2250. https://doi.org/10.1021/nl101260j
23. Bianchi M, Guan D, Bao S, Mi J, Iversen BB, et al. 2010. Coexistence of the topological state and a two-dimensional electron gas on the surface of Bi_2Se_3. *Nat Commun* 1(1): 128. https://doi.org/10.1038/ncomms1131

24. Hong SS, Cha JJ, Kong D, Cui Y. 2012. Ultra-low carrier concentration and surface-dominant transport in antimony-doped Bi_2Se_3 topological insulator nanoribbons. *Nat Commun* 3(1): 757. https://doi.org/10.1038/ncomms1771

25. Chen H, Zhu W, Xiao D, Zhang Z. 2011. CO oxidation facilitated by robust surface states on Au-covered topological insulators. *Phys Rev Lett* 107(5): 056804. https://doi.org/10.1103/PhysRevLett.107.056804

26. Liu CW, Wang Z, Qiu RL, Gao XP. 2020. Development of topological insulator and topological crystalline insulator nanostructures. *Nanotechnology* 31(19): 192001. https://doi.org/10.1088/1361-6528/ab6dfc

27. Kong D, Randel JC, Peng H, Cha JJ, Meister S, et al. 2010. Topological insulator nanowires and nanoribbons. *Nano Lett* 10(1): 329-333. https://doi.org/10.1021/nl903663a

28. Iyengar SA, Puthirath AB, Swaminathan V. 2023. Realizing quantum technologies in nanomaterials and nanoscience. *Adv Mater* 35(27): 2107839. https://doi.org/10.1002/adma.202107839

29. He QL, Hughes TL, Armitage NP, Tokura Y, Wang KL. 2022. Topological spintronics and magnetoelectronics. *Nat Mater* 21(1): 15-23. https://doi.org/10.1038/s41563-021-01138-5

30. Cha JJ, Koski KJ, Cui Y. 2013. Topological insulator nanostructures. *Phys Status Solidi Rapid Res Lett* 7(1β2): 15-25. https://doi.org/10.1002/pssr.201206393